Part III
Impact Injury Mitigation

Computer Simulation of the Skier-Flex Pole Impact in Slalom

Kurt Schindelwig, Peter Kaps, and Werner Nachbauer

Abstract In skiing the skier-flex pole impact causes a deflection and rotation of the flex pole and a speed loss of the skier. The purpose of the present study was to investigate the effects of skier and pole parameters on time loss, pole deflection, and pole damage speed caused by the skier-pole impact in slalom. Validated finite element models were used for the simulation of the impact. Skier mass, speed and impact height and pole mass, bending stiffness, diameter, and wall thickness were analyzed. Time loss was assessed for seven pole impacts by a simple simulation model of a skier schussing down an inclined plane. From the skier parameters, impact height followed by impact speed showed the highest effect on the skier-pole impulse. The impulse increased with increasing pole mass whereas the effect of bending stiffness was negligible. Time loss could be reduced by lowering the pole mass. However, lowering of pole diameter or wall thickness increased pole deflection enhancing injury risk due to the whiplash effect. Additionally, the reduction of wall thickness decreased pole damage speed with the disadvantage of higher risk of pole fractures. Overall, lowering pole mass for the current impact speeds in World Cup slalom races requires additional investigation. In children and youth races with lower impact speeds than in World Cup races, a pole mass reduction would be possible.

Keywords Flex pole • Slalom • Time loss • FE model • Safety aspects • Impact

1 Introduction

According to the competition rules of the International Ski Federation World Cup skiers hit about 130 flex poles during a slalom race [1]. Specifications for flex poles were developed by the FIS to guarantee that flex poles behave in the same manner

K. Schindelwig (✉) • W. Nachbauer
Department of Sport Science, University of Innsbruck, Innsbruck, Austria
e-mail: kurt.schindelwig@uibk.ac.at

P. Kaps
Department of Engineering Mathematics, University of Innsbruck, Innsbruck, Austria

I.S. Scher et al. (eds.), *Snow Sports Trauma and Safety*,
DOI 10.1007/978-3-319-52755-0_10

all over the world, to avoid injury caused by the pole impacts as much as possible, and minimize the risk of pole fracture so that a flex pole is operational over a period of at least 3 years (ca. 8000 passes) [2].

The resistance of the flex pole during impact leads to a speed loss and in consequence to a time loss of the skier. Innerhofer and Nachbauer [3] reported that skiers of low body mass and height have a competitive disadvantage compared to heavier and taller skiers. This disadvantage was more pronounced the more mass and height differed, e.g., speed loss per pole contact was reduced 23% by increasing body mass from 40 to 90 kg and reduced 27% by increasing impact height from 0.6 to 1.2 m.

The impact of the skier causes a deflection of the flex pole that may cause injury to the skier. As a result of the very fast acceleration of the upright pole by the skier impact, the tip of the pole rebounds shortly and may hit the skier in the head-shoulder-back area. This effect—in skiing referred to as the whiplash effect—is stronger for an upright pole with lower bending stiffness and higher mass. There are no injury data available for the whiplash injury mechanism. Bere et al. [4] analyzed 69 injury cases of the alpine skiing World Cup. Gate contact was assumed to contribute directly and/or indirectly to injury in 21 cases. Impacts that contributed indirectly to injury influenced the skier's balance leading to falls. Two injuries were reported for slalom. However, only severe injuries were analyzed.

Pole fracture data was not published. According to informal reports of coaches and pole manufacturers pole impacts by a skier causes fractures in the middle part of the pole and pole impacts to the ground create fractures in the tip region of the pole. Pole fractures during training/competition shorten the training time or extend the competition time. Moreover, flex poles are relatively expensive. In order to avoid fractures in the tip region, some manufactures attach an additional shell inside the upper end of the pole increasing wall thickness. To prevent injuries due to broken poles, FIS requests a ductile fracture behavior to ensure that the pole only snaps without breaking off completely [2].

In the study of Innerhofer and Nachbauer [3], the pole was modeled as a bending beam. The impact was modeled as pure elastic and pole deflection was taken from video images. Accordingly, plastic deformation was not considered. Schindelwig et al. [5] developed a finite element (FE) model of a flex pole. The model was validated using a pendulum impactor. Measured and simulated data correlated well with less than 2% difference for the impulse and 1.2% difference for the pole deflection.

Lighter and smaller racers have a considerable disadvantage in competitions due to pole resistance. A reduction of the resistance lessens the disadvantage; however, it may increase injury risk and pole fractures. Thus, the purpose of the present study was to investigate the effects of skier and flex pole parameters on time loss, pole deflection, and pole damage speed caused by the skier-pole impact in slalom.

2 Methods

2.1 Finite Element Modeling and Simulation

The applied finite element (FE) model of the flex pole was described in Schindelwig et al. [5]. The upright pole was discretized with S4R general quadratic membrane shell elements. Isotropic elastic and plastic material behaviors were used. The bending device was modeled by bushing connector elements with linear elastic behavior. A horizontally moving impactor was used to reproduce the impact by the skier. The impactor was modeled as a cylinder with a diameter of 0.1 m and a length of 0.2 m. Contact with the flex pole occurs mostly with the ski pole or with the guard of the ski pole (Fig. 1). Since the ski pole is often made of aluminum, an aluminum cylinder was used for the impactor. Isotropic elastic material behavior with a typical Young's modulus for aluminum of 69 GPa [6] was used for the solid extrude elements. The impact mass was set to the skier's mass. Videos recorded with a high-speed camera (frame rate 200 fps, Sony NEX-FS700K, Sony, Tokyo, Japan) of two women and two men World Cup slalom races in the 2014/15 season showed that the impact height was in average 44% of the skier's height. Accordingly, impact height of the first contact between impactor and flex pole was set to 44% of the skier's height.

The FE simulations were performed in an explicit dynamic analysis using Abaqus explicit 6.12–1 (SIMULIA, Dassault Systèmes, Providence, Rhode Island, US). For element types, the settings "standard" from the element library and "reduced integration" were selected. The normal behavior was used for the contact properties with the "Hard" contact for the pressure-overclosure. Based on the analysis of the above-mentioned high-speed videos ground contact of the pole occurred about 0.1 s after initial pole contact. Thus, simulations were stopped after 0.1 s.

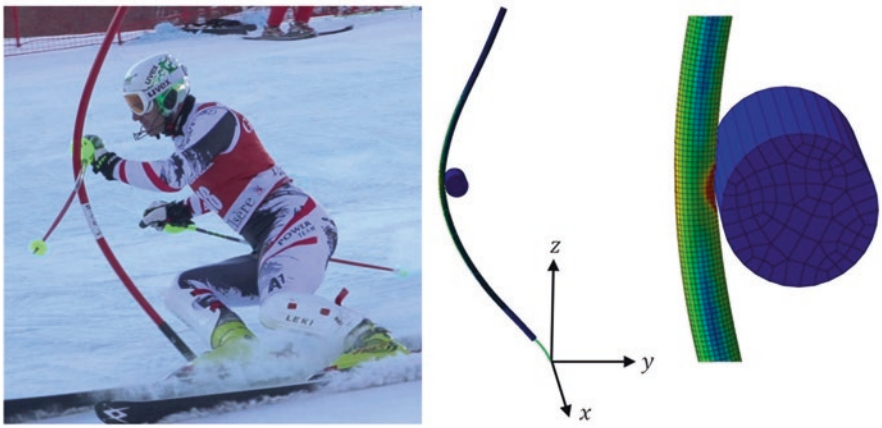

Fig. 1 (*Left*) picture of the skier-flex pole impact, schematic illustrations of the FE model's flex pole and impactor: (*center*) overall representation with coordinate system and (*right*) flex pole and the impactor in detail

2.2 Impulse and Speed Loss

The impulse p was calculated by the speed loss Δv of the impact cylinder and its mass m with $p = m \bullet \Delta v$. The speed loss Δv of the impact cylinder was determined by the FE simulations for varied skier and pole parameters. Impact height was varied in increments of 0.1 m from 0.3 to 1.6 m, impact mass in increments of 10 kg from 30 to 90 kg, and impact speed in increments of 1 m/s from 5 to 21 m/s. Pole mass was varied in increments of 100 g from 200 to 800 g by changing pole density. Bending stiffness was varied in increments of 10 Nm^2 from 20 to 80 Nm^2 by changing Young's modulus. Only one parameter was varied while the others were kept constant as follows: pole diameter 31 mm (d31), wall thickness 3 mm (w3), body mass 90 kg, impact height 0.84 m (skier "Tall", Table 1), impact speed 13 m/s, pole density 1160 kg/m^3, and pole length 1.74 m.

Additionally, all combinations of pole diameters of 25, 27, 29, and 31 mm and wall thicknesses of 2, 2.5, and 3 mm were analyzed. The chosen pole diameters were within the limits of 25–32 mm requested by the FIS [2]. Pole mass was calculated from diameter d, wall thickness w, length l, and densitiy ρ of the pole with

$$m_{up} = \left(d \cdot w - w^2\right) \cdot \pi \cdot l \cdot \rho.$$

Young's modulus was set to 2.45 GPa for all poles [5]. Bending stiffness B_{up} was calculated from diameter d, wall thickness w, and Young's modulus E with

$$B_{up} = E \cdot \left(\frac{d^4 - \left(d - 2 \cdot w\right)^4}{64}\right)$$

2.3 Time Loss

Speed loss Δv of the impact cylinder was obtained by the FE simulation. From speed loss per impact, time loss for seven pole impacts during a straight run on inclined planes of 5° and 20° was calculated. For this, the equation of motion of a mass point with initial speed of 13 m/s, gliding distance of 42 m, and coefficient of snow friction 0.02 was solved. The drag for the skier "Tall" was set to 0.6 m^2 according to wind tunnel measurements [7]. Drag was decreased proportional to the mass of the skiers "Small" and "Medium" (Table 1) to 0.2 and 0.4 m^2 so that the acceleration of the three skier types was identical and time loss was only caused by the skier-pole impacts. The speed of a skier after impact was set to the speed before impact minus speed loss.

Table 1 Body mass, body height, and impact height of the skiers "Small," "Medium," and "Tall"

Skier	Small	Medium	Tall
Body mass (kg)	30	60	90
Body height (cm)	130	160	190
Impact height (cm)	58	71	84

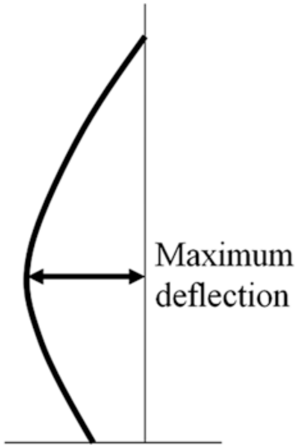

Fig. 2 Schematic illustration of the maximum deflection

2.4 Pole Deflection

The FE simulation provided the 3D coordinates of 35 nodes along the pole in increments of 5 cm from initial pole contact to ground contact. From the 3D coordinates, the maximum horizontal distance between pole tip and nodes of the pole of the first deflection phase in the running direction (Fig. 2) was determined. This distance was denoted as maximum deflection, which is a measure of the whiplash effect.

2.5 Pole Damage Speed

Pole damage speed was defined as the lowest impact speed causing a reduction of the pole diameter of more than 3 mm at 0.1 s after initial pole impact. Plastic deformation accounted for this diameter reduction. For the determination of the damage speed, the impact speed was increased in increments of 1 m/s starting with 8 m/s until an apparent damage occurred. To simulate an unfavorable load case impact height was lowered to 0.5 m (shin guard impact) and impact mass of 90 kg was chosen.

3 Results

3.1 Effect of Skier and Pole Parameters on Impulse

The largest effect on the impulse was observed for impact height followed by impact speed. By lowering impact height from 1.6 to 0.3 m the impulse increased from 4 to 35 Ns. The effect of body mass on the impulse was negligible. An increase of impact

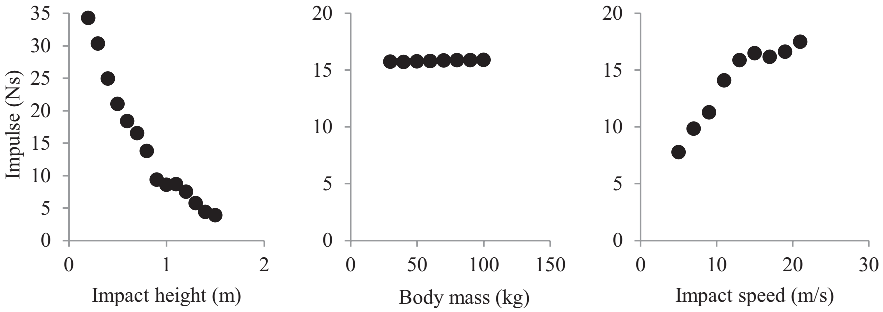

Fig. 3 Impulse for different (*left*) impact heights, (*center*) body mass, and (*right*) impact speeds (flex pole diameter 31 mm and wall thickness 3 mm (d31-w3))

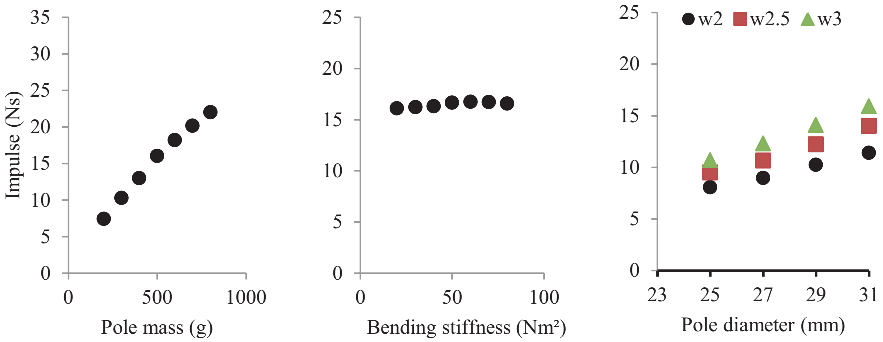

Fig. 4 Impulse for different (*left*) pole mass and (*center*) bending stiffness (skier "Tall"), and (*right*) pole diameter and wall thickness (w) (skier "Tall")

speed from 5 to 21 m/s resulted in an increase of the impulse from 8 to 18 Ns. This increase was nearly linear from 5 to 15 m/s; above 15 m/s almost no increase was observed (Fig. 3).

In Fig. 4, the effect of pole mass, bending stiffness, pole diameter, and wall thickness on the impulse are presented for the impact with skier "Tall." The increase of pole mass from 200 to 800 g caused an increase of the impulse from 8 to 22 Ns. Only minor changes of the impulse were observed for bending stiffness between 20 and 80 Nm^2. The impulse increased approximately linearly with pole diameter as well as with wall thickness (Fig. 4).

The variation of pole diameter and wall thickness varied pole mass and bending stiffness as listed in Table 2. Pole mass and bending stiffness ranged from 290 to 530 g and from 23 to 64 Nm^2.

Table 2 Pole mass and bending stiffness for different pole diameters and wall thicknesses. Material density was 1160 kg/m^3 and Young's modulus 2.45 GPa

Diameter (mm)	25	27	29	31	25	27	29	31	25	27	29	31
Wall thickness (mm)	2				2.5				3			
Pole mass (g)	290	320	340	370	360	390	420	450	420	460	490	530
Bending stiffness (Nm^2)	23.6	30.3	38.1	47.2	27.7	35.7	45.2	56.1	31.3	40.5	51.4	64.1

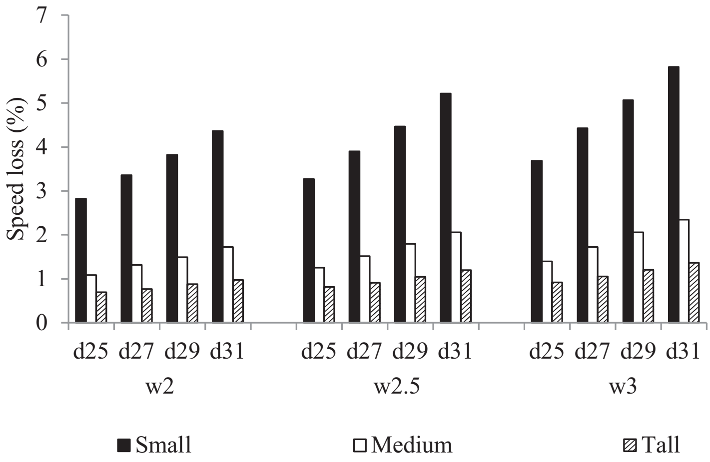

Fig. 5 Speed loss for skiers "Small," "Medium," and "Tall" by impact with different pole diameters and wall thicknesses

3.2 *Effect of Pole Diameter and Wall Thickness on Speed and Time Loss*

The highest speed loss of 5.8% was calculated for the impact of skier "Small" with the pole diameter 31 mm and wall thickness 3 mm (d31-w3). Reducing both the pole diameter from 31 to 25 mm and the wall thickness from 3 to 2 mm reduced speed loss to 2.8%. Speed loss for skier "Tall" with poles d31-w3 and d25-w2 was 1.4 and 0.7%, respectively (Fig. 5).

The running time without pole impacts for straight schussing on the 42 m slope with 5° inclination was 3.20 s. Seven impacts with d31-w3 resulted in time losses of 0.87, 0.29, and 0.16 s for the skiers "Small," "Medium," and "Tall,, respectively. These time losses were nearly halved for pole d25-w2. On the steeper slope of 20°, time losses were reduced to about 50% due to higher acceleration of the skiers. In Fig. 6, the time loss differences between the "Small" and "Medium" skiers and "Medium" and "Tall" skiers are presented for seven impacts on the flatter slope of 5°.

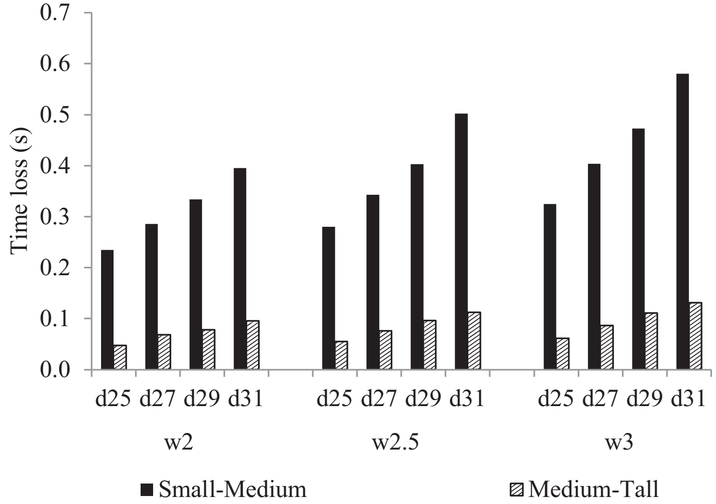

Fig. 6 Time loss differences of skiers "Small"–"Medium" and "Medium"–"Tall" caused by seven impacts during a straight run on a 42 m long slope with 5° slope inclination. Flex pole diameter and wall thickness were varied

Reducing both the pole diameter from 31 to 25 mm and the wall thickness from 3 to 2 mm reduced the differences of the time losses between skier "Small" and "Medium" from 0.58 to 0.24 s and between "Medium" and "Tall" from 0.13 to 0.05 s.

3.3 Effect of Pole Diameter and Wall Thickness on Pole Deflection and Pole Damage Speed

An increase of the pole diameter from 25 to 31 mm reduced the maximum deflection by about 0.1 m for all wall thicknesses for skier "Small" and "Medium". Therewas no effect observed of the pole diameter on the maximum deflection for skier "Tall" (Fig. 7 left). The effect of wall thickness on maximum deflection was small. The highest maximum deflection occurred for skier "Small" and the lowest for skier "Tall." The correlation between maximum deflection and impact speed was approximately linear with a gradient of 0.023 s (Fig. 7 right).

Pole damage speed increased clearly with decreasing pole diameter and increasing wall thickness. For the same wall thickness, a decrease of the pole diameter from 31 to 25 mm increased the damage speed from 10 to 16 m/s (w2), from 15 to 19 m/s (w2.5), and from 17 to 20 m/s (w3) for wall thickness of 2, 2.5 and 3 mm,

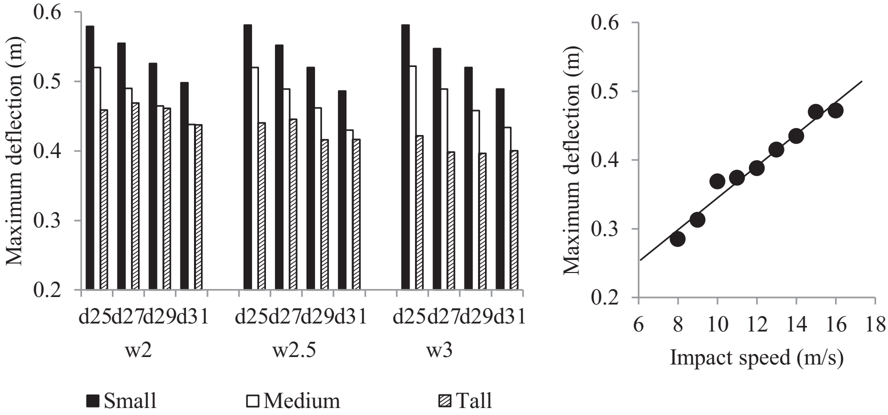

Fig. 7 Maximum deflection for skiers "Small," "Medium," and "Tall" (*left*) by impact with different pole diameters and wall thicknesses (impact speed 13 m/s), and (*right*) for impact speeds 8–16 m/s (skier "Tall" with pole d31-w3)

Table 3 Damage speed for different pole diameters and wall thicknesses (body mass 90 kg, impact height 0.5 m)

Diameter (mm)	25	27	29	31	25	27	29	31	25	27	29	31
Wall thickness (mm)	2				2.5				3			
Damage speed (m/s)	16	14	13	10	19	17	16	15	20	21	19	17

respectively. An increase of the wall thickness by 0.5 mm increased the damage speed between 2 and 3 m/s for the different pole diameters (Table 3).

4 Discussion

The effect of skier and pole parameters on the impulse between skier and pole was determined. For this purpose, skier parameters were varied in a range representatively for athletes of age 10 to adults. Pole parameters were varied reasonably adjusted beyond the limits permitted by the FIS specifications. The impact height of the skier showed the largest effect on impulse. The impulse was about nine times higher at 0.3 m than at 1.6 m. In addition, impact speed affected the impulse considerably. There was a nearly directly proportional relationship up to an impact speed of 15 m/s; above 15 m/s, impulse was independent of speed. Commonly, the skier-pole impact consisted of three successive contacts which were also detected in the high-speed videos from World Cup races. In the simulations, the durations of the three contacts were about 10, 5, and 14 ms for the flex pole d31-w3 and the second and third contact was about 39 and 55 ms after initial contact, respectively. At speeds up to 15 m/s almost two thirds of the impulse was generated by the second and third contact. At higher speeds, the first contact resulted in an increased inclination of the pole, reducing the impact during the second and third contact and causing the described speed independency. Unexpectedly, the impulse was nearly independent of the skier's mass. The reason for the independence is the low ratio of the pole mass (500 g) to the skier's mass. The ratio was lower than 1/60 for the analyzed skiers. The independence of the impulse from the skier's mass leads to an indirectly proportional relationship between mass and speed change of the skier. A reduction of the mass by half doubles the speed loss of a skier.

The impulse was strongly affected by pole mass in a directly proportional manner while the effect of bending stiffness was negligible. For the variation of pole mass and bending stiffness unrealistic values of pole density and Young's modulus were assumed. Mass and bending stiffness of poles are strongly influenced by pole geometry, which is given by diameter, wall thickness, and length. Since geometry affects both mass and bending stiffness, it is in reality not possible to vary one without altering the other. However, the impulse changes presented for different pole diameters and wall thicknesses by keeping the material properties constant were mainly caused by changes of the pole mass. For instance, pole d25-w2 had half the mass of pole d31-w3, consequently, also the impulse of the pole d25-w2 was half of the pole d31-w3.

Speed loss was calculated through simulations of impacts between different poles and skiers classified as "Small," "Medium," and "Tall." To assess the practical relevance of the speed loss in a slalom competition, the time loss of four 42 m long flat course sections with seven pole contacts each (two sections per slalom run) was calculated. These calculations revealed that, as compared to skier "Medium," skier "Small" would lose 0.86 and 2.32 s for poles d25-w2 and d31-w3, respectively. In children's races, body weight and height may differ by a magnitude similar to that between the skiers "Small" and "Medium" considered in our simulations. Assuming a 5.6 s time difference between rank 1 and 10 (average of six children mastership races) [8], the skier "Small" would lose four positions in the ranking using pole d31-w3 but only one position using pole d25-w2. In World Cup races, usage of pole d31-w3 (World Cup standard) results in a time difference of 0.56 s between skiers "Medium" and "Tall." This is equivalent to a competitive disadvantage of two positions.

The results revealed that from a view of fairness the reduction of the pole mass would be beneficial. Since the density of polycarbonate lies in a narrow range, mass reduction can only be accomplished by lowering pole length, pole diameter, and/or wall thickness. The reduction of pole length from 1.8 to 1.6 m was realized in Austria for children competitions younger than 12 years [9]. For children of age 12 and older a length reduction was in discussion, however, it was discarded due to the risk of fascial injury through contact with the tip of the pole. Lowering of pole diameter or wall thickness increases maximum pole deflection, which enhances injury risk since the upper pole may hit the skier at the head-trunk area due to the whiplash effect. Moreover, a reduction of wall thickness decreases pole damage speed, which increases the risk of pole fractures. For the current impact speeds in World Cup slalom races, advanced investigations are necessary for lowering the pole mass.

In children and youth races, skiing speed and thus impact speed is clearly lower than in World Cup races resulting in lower skier-pole impulse with lower maximum pole deflection and pole damage speed. Lower speeds permit reducing pole mass by lowering pole diameter and wall thickness. Assuming lower impact speeds of 2 m/s than in World Cup races, pole d27-w2.5 showed the same maximum deflection as the World Cup approved pole d31-w3. Also the difference between impact speed and pole damage speed was the same for both poles. However, time loss would be reduced about 40% in the described seven gate flat course due to the mass reduction.

5 Limitations

In this study, variations of temperature or plasticity of the upright pole were not considered. A yielding movement of the skier at pole contact was not included. The dimension of the impactor was not varied. An impactor with a smaller diameter may reduce damage speed. Pole damage speed was not analyzed for the impact on the snow surface.

Acknowledgments The authors would like to thank the International Ski Federation for its financial support. The computational results presented have been achieved using the HPC infrastructure LEO of the University of Innsbruck.

References

1. The International Ski Federation (FIS) (2014) The international ski competition rules (ICR) Book IV Joint regulations for alpine skiing. http://www.fis-ski.com/mm/Document/documentlibrary/AlpineSkiing/03/29/54/ICR_clean_12082014_Neutral.pdf. Accessed 19 Sep 2016
2. The International Ski Federation (FIS) (2008) FIS specifications for flex poles. http://bmsi.ru/media/75f004dd-d384-4d1f-aa99-0882bff649b3/kip08e.pdf. Accessed 12 Nov 2015
3. Innerhofer G, Nachbauer W (1999) Influence of the skier's mass and height on clearing slalom gates. Paper presented at the 10th European congress on sports medicine, University of Innsbruck, Innsbruck, 22–24 September 1999
4. Bere T, Flørenes TW, Krosshaug T, Haugen P, Svandal I, Nordsletten L, Bahr R (2013) A systematic video analysis of 69 injury cases in World Cup alpine skiing. Scand J Med Sci Sports 24:667–677
5. Schindelwig K, Ellensohn S, Kaps P, Nachbauer W (2016) Validation of a 3D finite element model for flex pole impacts. JSET (in review)
6. Gall K, Horstemeyer MF, Degner BW, McDowell DL, Fan J (2001) On the driving force for fatigue crack formation from inclusions and voids in a cast A356 aluminum alloy. Int J Fract 108:207
7. Brownlie L, Larose G, D'Auteuil A, Allinger T, Meinert F, Kristofic P, Dugase S, Boyde R, Stephens D (2010) Factors affecting the aerodynamic drag of alpine skiers. Procedia Eng 2:2375–2380

8. The International Ski Federation (2016). http://www.fis-ski.com/alpine-skiing/events-and-places/results/. Accessed 13 Apr 2016
9. Austrian Ski Federation (2016). https://www.oesv.at/media/media_vereinsservice/media_wettkampfordnungen/OeWO-ALPIN-2015-2016-fuer-Homepage.pdf. Accessed 13 Apr 2016

Sagittal Plane Helmet Acceleration at Pole Contact of Alpine Ski Racers is Dependent on Slalom Pole Type and Skill Level

Ronald W. Kipp and John G. Seifert

Abstract A slalom ski racer's center-of-mass (CoM) has a negative acceleration during a turn. Some of this change in acceleration can be attributed to the physical contact with the pole, and possibly physiological and/or psychological factors of the ski racer. One factor may be the type/size of poles (gates) used to define the race line (route prescribed by competition rules) in slalom. Poles come in a variety of sizes and styles. This study utilized five differing pole types with 12-year-old male and female racers. As a general conclusion, they were faster on the small/shorter poles. They also felt faster, more aggressive, higher level of confidence, and thought their race line was superior on the shorter poles. When looking at the acceleration component, we divided the skiers into "skilled" and "less skilled." The two groups differed on direction of acceleration. The discussion lays out mechanical, physiological, psychological, and technique ramifications to interpret this acceleration paradox.

Keywords Ski racers • Slalom • Pole contact • Head injury • Pole design

1 Introduction

1.1 Acceleration

Alpine ski racers ski around poles which are used to describe the race line. Each ski turn creates a situation where there is a negative acceleration of the skier's center-of-mass (CoM) followed by a period of positive acceleration between turns [1]. To ski fast in slalom, the ski racer skis with their skis close to the pole such that their CoM may actually travel to the inside of the race line. This is a legal passage according to the rules of the Fédération Internationale de Ski (FIS), the governing body of international ski racing. Racers will contact the long pole hitting, blocking, moving,

R.W. Kipp (✉)
United States Ski and Snowboard Association, Park City, UT, USA
e-mail: ronwadekipp@gmail.com

J.G. Seifert
Movement Science Laboratory, Montana State University, Bozeman, MT, USA

I.S. Scher et al. (eds.), *Snow Sports Trauma and Safety*,
DOI 10.1007/978-3-319-52755-0_11

or clearing it out of the way with their hand and or ski pole, allowing their body to take a shorter path. This pole contact and movement requires about 181 J for each pole clear for a World Cup ski racer which may explain part of their CoM-negative acceleration (R. Reid, personal communication, 2010). This negative acceleration would be amplified for young skiers having less mass.

While ski racers must ski around poles, recreational skiers make turns in voluntary locations and tempo. For recreational skiers, turning is an opportunity to manage speed while for the ski racer it is a situation for speed loss to be minimized.

1.2 Poles and Training Aids

Poles are used in alpine ski racing to define the race line for the ski racer. The FIS [2] has specifications for pole dimensions used in international competition, while individual countries determine domestic standards.

Poles have a hinge at the snow level. This hinge was developed to keep the pole from becoming dislodged as ski racers skied increasingly closer to the pole eventually discovering they could just mow down the pole with their hand, ski pole, or shin enabling them to take a shorter and therefore faster path. Standards for the hinge are mandated by the FIS.

The FIS has two categories of poles: Type A; which is for use in any FIS race. They have a shaft diameters from 29 to 32 mm. Type B poles (25–28.9 mm) are for use in any FIS race except World Cup.

Poles vary by their height above the snow surface. All FIS races must employ poles that project a minimum of 1.8 m above the snow surface [3]. In the United States, U16 competitions must also use the 1.8 m poles (FIS A or B). However, slalom poles for U14s must be 152 cm FIS B, while stubby poles are for non-scored events [4].

Young ski racers typically compete with shorter length (137 and 152 cm) and smaller diameter poles (27 vs. 32 mm). In place of poles, props or training aids, such as Whiskers and Heroes, reduce contact while still skiing the intended path. Whiskers are 23 cm brushes and Heroes are 70 cm flexible poles. There are no FIS standards for Whiskers and Heroes (SPM S.P.A., Varese, Italy).

The purpose of this study was to determine if pole type or shaft length had an effect on acceleration. Additionally, would finishing time, and subjective feelings of young ski racers be altered by pole length?

2 Methods

2.1 Subjects

Eighty seven (54 females, 33 males) club level skiers from three different USSA (United States Ski and Snowboard Association) affiliate ski teams participated in the study. Data are presented as average (± standard deviation). Average age was

12 years 10 days (±1.0 year). Skiers reported an average 4.6 (±0.9) years of race experience. Average height was 153.4 (±8.9) cm, average weight 41.05 (±10.88) kg, and average ski length was 140.4 (±7.80) cm. "Skilled" and "unskilled skiers" were defined by the nine skiers with the fastest and slowest run time. This was then confirmed with video by a USSA-certified ski coach.

2.2 Courses

The study was conducted on 12 different slopes at Bridger Bowl Ski Area, Montana, and Park City Mountain Resort, Utah, over 11 separate days in winter conditions. The 12 slopes averaged 20.9 degrees (±2.7). They were relatively even in pitch with minimal side hill. Individual average pitches consisted of 20, 23.5, 28, 22, 22, 18, 18, 20, 20, 19.4, 20, 20°.

An identical ten gate slalom course was set for all trials. It consisted of four open gates set at 9 m (gate to gate) to a three gate flush at 5.5 m followed by three open gates set at 9 m (gate to gate) to the finish 9 m away (see Fig. 1). Offset was 4 m with the flush in line with the same 4 m horizontal distance. All courses were slipped frequently in order to minimize rut development and overall course deterioration.

Skiers completed one or more runs on each pole type course in a random order. Multiple runs on the same course were used to check for reliability between runs.

Fig. 1 Course set-up used for all data collection

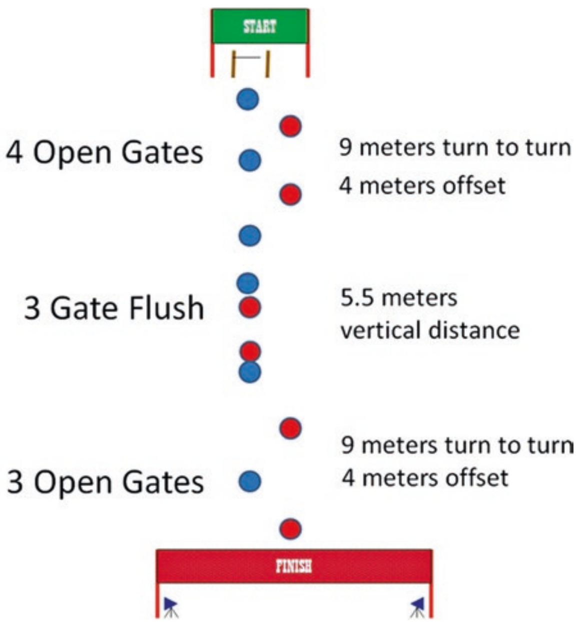

2.2.1 Pole Type Used During Each Testing

- Whiskers: Bright orange and green plastic were alternated in the courses. 23 cm length, with a lightly threaded 20.5 cm base.
- Hero: Red and blue, pliable, rubber-like shaft, 35 mm in diameter and 70 cm long. 86 cm overall length including BrushGrip™ Base.
- 137 cm: 27 mm diameter shaft that is 137 cm off the snow with BrushGrip™ Base.
- 152 cm: 27 mm diameter shaft that is 152 cm off the snow with BrushGrip™ Base.
- 180 cm: 27 mm diameter shaft that is 180 cm off the snow with BrushGrip™ Base.

All poles, Heroes, and Whiskers were manufactured by *SPM* and were new at the beginning of the study. Pole hinges showed no sign of deterioration at the end of the study.

2.2.2 Timing

The order in which the courses were skied was randomized for each testing bout.

Timing was with a Brower XS Timing System (Salt Lake City, UT, USA).

2.2.3 Acceleration

A gyroscopically controlled three-dimensional accelerometer (Electronic Realization, Bozeman, MT) was attached to the crown of the skier's helmet. Sagittal plane, the fore/aft direction was defined as "x" the vertical direction as "y" the lateral direction as "z".

2.2.4 Skier Perception

Skier perception immediately at the conclusion of each run was collected. The subject responded to four statements indicating their perception about speed, aggressiveness, confidence, and line with a 10-point Likert scale.

On that course I felt:

- Slow…fast
- Not aggressive…very aggressive
- Not confident…very confident
- Not a good line…a very good line

The higher the response number, the more positive the skier felt. A single factor ANOVA and post hoc Tukey HSD were used to calculate significance.

3 Results

3.1 Time

For the analysis 522 valid runs were used.

Average run time and standard deviation (SD) in seconds per pole type (Table 1): Statistically (single factor ANOVA and post hoc Tukey HSD):

- Whiskers and Heroes times are not different from each other.
- Whiskers and Hero times are different from 137 cm, 152 cm, 180 cm ($p = 0.01$).
- 137 cm and 152 cm times are not different from each other.
- 137 cm and 152 cm times are different from Whiskers, Heroes ($p = 0.01$), 180 cm ($p = 0.01$, $p = 0.05$).
- 180 cm times are different from all other poles ($p = 0.01$), 137 cm ($p = 0.05$).

3.1.1 Reliability Between Runs of Same Pole Type (Within Skier)

Determining the variability between run times was important to establish test-retest reliability. 141 duplicate runs from the five pole/training aids were used to determine reliability. One factor to be noted was that the runs used were all from the same measurement day. Due to the multivariate nature of ski racing, this was the best option to control for the many variables that would most likely change from day to day.

A very high reliability [Pearson Product-Moment Correlation coefficient (r)] was found for all pole and training aid types (Table 2):

Table 1 Average run time ± SD (s) per pole or training aid type

	Average	SD
Whiskers	11.810	1.652
Hero	11.769	1.981
137 cm	12.644	1.772
152 cm	12.502	1.600
180 cm	13.011	1.770

Table 2 Reliability for each pole and training aid type

	r
Whiskers	0.953
Hero	0.991
137 cm	0.978
152 cm	0.956
180 cm	0.948
Average	0.967

3.2 Perception

Skiers showed consistent trends in perception after their conclusion.

3.2.1 Questionnaire Results (Table 3)

3.3 Acceleration

3.3.1 Mean Acceleration Skilled vs. Less Skilled

There were significant differences for mean sagittal plane helmet acceleration between the three pole types and the two training aids. Also, a significant difference was observed when the skiers were grouped into "skilled" and "less skilled" cohorts ($p = 0.0000$). The skilled skiers having a positive acceleration while the less skilled a negative acceleration. See Fig. 2.

Table 3 Results from the 0–10-point Likert scales asked at the conclusion of each run

	Slow/fast	Aggressiveness	Confidence	Line
Whiskers	8.04	8.25	8.46	7.90
Hero	7.85	7.97[a]	8.57	7.80
137 cm	7.80	7.99	8.49	7.92
152 cm	7.97	8.06	8.15[b]	7.54[c]
180 cm	6.99[d]	7.31[d]	7.58[d]	6.91[d]

[a]Significantly different from Whiskers ($p = 0.05$)
[b]Significantly different from 137 cm and Heroes ($p = 0.01$)
[c]Significantly different from 137 cm ($p = 0.01$) and Whiskers ($p = 0.05$)
[d] Significantly different from all other poles and training aids ($p = 0.01$)

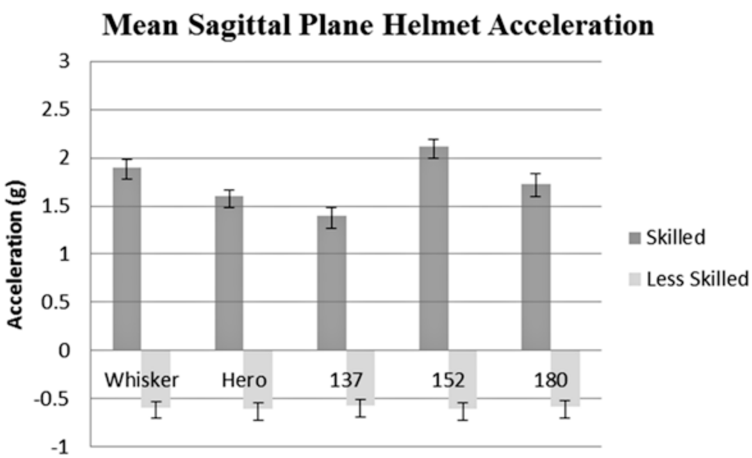

Fig. 2 Helmet acceleration across pole type

There was also a significant difference in mean acceleration between the skilled and less skilled in the vertical ($p = 0.000$) and lateral ($p = 0.000$) directions.

There were no significant differences in mean acceleration in any of the three directions between the five pole types, nor was there any difference when grouped into the two training aids (Whisker and Hero) and the two longer pole lengths (152 and 180 cm) for any of the three directions. See Fig. 3.

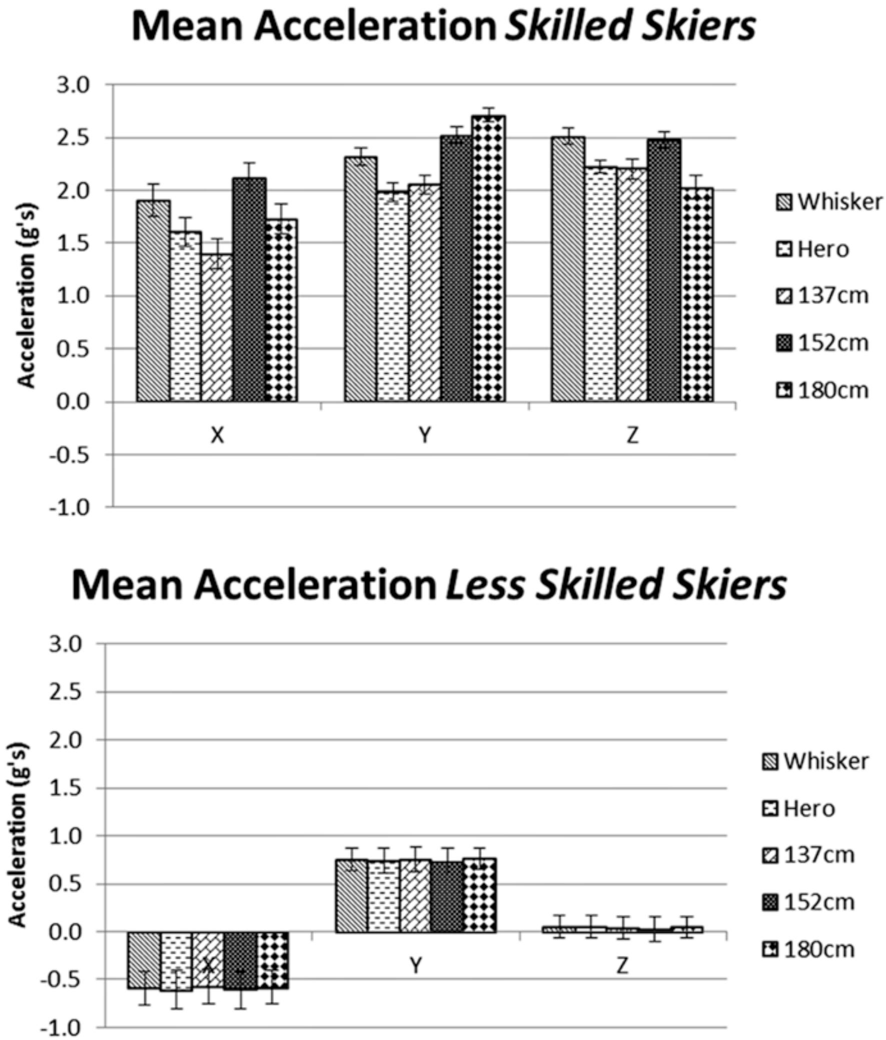

Fig. 3 Mean accelerations in the fore/aft (x), vertical (y), and lateral (z) direction for the three pole lengths and two training aids for skilled and less skilled ski racers

3.4 Peak Acceleration

When averaged over ten consecutive turns there was significant differences for peak acceleration for the skilled group in the z direction ($p = 0.03$) when the short props were compared to the two long poles, and for the less skilled in the y direction ($p = 0.05$). When the short props were compared to the two long poles, all other short props vs. tall poles were nonsignificant.

4 Discussion

Three pole types (lengths) and two training aids were selected for this study. The 27 mm shaft diameter was chosen over the 25 mm shaft based upon a previous USSA club questionnaire and US supplier recommendations. The 137 and 152 cm lengths were chosen as they are popular lengths used in the United States for young ski racers, and 180 cm as the FIS standard. Whiskers and Heroes were included as they are popular training choices.

The subjects were very homogenous in age. The control of age was important to eliminate or reduce age as an extraneous variable that could potentially affect the results. The study was conducted over 11 nonconsecutive days on 12 differing slopes. This helped to ensure that the results would be representative to the population in question.

Acceleration was positive for the skilled skiers and negative for the less skilled skiers across all three pole lengths and the two training aids. The question must be asked, was this difference in acceleration due to the pole length or type, or was it indicative of the skilled behavior?

Did pole type effect time? Whisker and Heroes were the fastest, with the 137 and 152 cm next, followed by 180 cm as the slowest. This time transition from shorter pole to longer pole agrees with intuitive logic and could be based on the mechanical energy dissipation consequence of shaft deformation, shaft acceleration, and hinge resistance, or possibly the influence of pole size on the racer's psychological state.

The run time of Whiskers and Heroes were not statistically different from one another. Contact with the pole or any line alteration with the Hero did not seem to influence the finish time when compared to the Whiskers. This was confirmed with the skier's subjective impression giving a similar response (Whisker: 8.04, Hero: 7.85) when asked if they felt "slow" (0) or "very fast" (10). The skiers also report feeling less aggressive on the Hero (7.97) courses than the Whisker (8.25) courses ($p = 0.01$).

The 137 and 152 cm poles were not significantly different from each other in time. However, they were significantly different from the Whisker, Hero, and 180 cm. While the skier's time was not statistically different, they did report feeling less confident and less satisfied with their line when skiing the 152 cm pole.

The 180 cm poles elicited the slowest time, which was also the feeling generated from the skiers. The skiers also felt less aggressive and less confident along with less satisfaction with their line.

A very high reliability was found for all five pole types (cumulatively $\underline{r} = 0.967$). Reliability is an essential component of validity which was essential for this study. Being assured that a run time per pole type was indeed indicative of that pole type was crucial to the interpretation of the results.

4.1 Possible Explanations

There are natural acceleration consequences of a skier center-of-mass during a ski turn. Reid and coworkers have used kinematic data with elite ski racers showing that during a slalom turn, the skier's CoM goes through a period of negative acceleration that is followed by a period of positive acceleration between turns [1]. The period of negative acceleration starts when the turn is initiated which is before flex pole contact. Recently, Schindelwig and coworkers used finite element analysis to demonstrate the increase in race time due to a longer flex pole in children's slalom racing [5].

4.1.1 Physical Contact with the Pole

It has been calculated that elite ski racers contacting an FIS A pole will use 45 J for work to deform the pole, 108 J to accelerate the pole, and 28 J to overcome hinge resistance for 181 J of work. This comes out to be about 4% of his kinetic energy (R. Reid, personal communication, 2010). Upon video analysis, the less skilled skiers did not necessarily contact the pole.

4.1.2 Anticipatory Postural Control

Racers contact the pole by hitting, blocking, moving, or clearing it out of the way with their hand or ski pole allowing their body to take a shorter path. The action to perform this "clearing" maneuver involves raising the arm which is accomplished with the pectoralis major and anterior fibers of the deltoid. While this is the mechanism, a phenomena observed and described by Belen'kii et al. [6] that standing subjects when asked to raise their arm, utilized both their prime movers (arm) and their postural muscles (trunk and legs). The postural muscles innervate 50 ms prior to the prime mover activation. This was in anticipation the upcoming destabilizing effects of the arm movement.

The more skilled ski racers could be anticipating the impact of pole contact with their postural muscles. These could be with the lower body or the neck muscles. In such a case, they are accelerating their upper body in proactive manner intuitively knowing that the pole will have a negative accelerating effect on them. This anticipatory postural adjustment has been shown to be a learned response by Cordo and Nashner [7]. The less skilled ski racers may not have had ample experience to have sufficiently learned this anticipatory postural mechanism and partially explain the resultant negative acceleration seen in this study.

4.1.3 Vestibulo-Ocular Reflex

The vestibulo-ocular reflex (VOR) maintains the visual image during linear and angular head movement. While skiing skill may be thought of as the ability to manipulate the skis in an efficient strategy, there may be an adaptive mechanisms in the central nervous system that is important in maintaining the VOR [8, 9]. This adaptation may be a result of increasing skiing skill or possibly a manifestation of maturity.

VOR motor learning functions to improve motor performance. This occurs via the gain of the VOR or the ratio of eye to head speed and its phase which is the temporal relationship between eye and head movement. Eye movements are opposite in direction and approximately equal in speed to the head movement [10]. It could be postulated that the positive acceleration from the skilled skiers at pole contact was an anticipatory learned response knowing that the pole would provide some negative acceleration at contact.

4.1.4 Psychological Factors

One explanation for the positive and negative acceleration at pole contact from the skilled and less skilled can be explained by the novelty of situation. The skilled skier has encountered this situation many times and knows what to expect. The less skilled skier is not as sure what to expect. The less skilled skiers' negative helmet acceleration may be a result of moving away from the pole in a ducking or avoidance response.

4.1.5 Ski Pressure Management

Elite ski racers strive to pressure their skis while they are in the fall-line or in the part of the turn that is pointed down the hill. Less skilled ski racers and recreational skiers that are striving for speed control as opposed to speed conservation will have pressure later in the turn. This type of turn will not accelerate in the turn but constantly show a negative acceleration throughout the turn.

4.1.6 Movement Decision Under Risk

Alpine skiing can be perceived as a risky endeavor. The skier skill level can lead to behavior that is based on risk avoidance or risk-seeking objectives [11, 12]. A risk avoidance situation can be postulated from the less skilled ski racers that will have greater variability in most aspects of their skiing technique suggesting increased instability [13]. Some of the negative acceleration seen in this study could be explicated by the risk perception that occurs during the middle of the turn when the skis are pointed at their most down the hill attitude and coinciding with a possible pole contact. Both could be assumed to be a "risky" moment in time.

4.2 What Does It Mean for Safety?

There are many ways to become injured skiing. The most obvious is losing some level of control of the skis. When injury does happen, there is a 50% chance it is to the lower extremity, which today usually means an ACL injury [14, 15]. Most of the ACL injuries among recreational skiers are reported to occur during falling [16, 17]. The three mechanisms of ACL injury all involve falling either in a backward or a forward direction. [18]. Specifically, the "phantom-foot," "boot-induced anterior drawer," "slip-catch," "landing back-weighted," and the "dynamic snowplow" mechanisms all have the skier falling backwards while the "valgus-external rotation" the skier falls forward. This is different from the mechanisms for other sports, such as American football, basketball, and soccer. In these activities, the foot is in firm contact with the ground and usually results in deceleration, change-of-direction, or some sort of direct blow. In skiing, the skis are constantly sliding forward while not in contact with the ground. This forward motion constantly challenges the skier to maintain control of their fore/aft relationship.

Fore/aft balance has always been a nemesis to the skier. The importance to recreational skiers is that the Professional Ski Instructor's of American lists "controlling the relationship of the center-of-mass to the base of support to direct pressure along the length of the skis" as one of their five Fundamentals of Skiing [19]. And among elite ski racers, fore/aft movement has been found to be correlated with speed in a race course [20, 21].

While it would be inappropriate to suggest that having superior fore/aft balance would lead to greater control, and therefore greater safety, it would conversely be irresponsible to overlook the relevancy and connection between sagittal plane control and the possible association with safety.

Acknowledgements World Cup Supply, VT, USA for supplying new SPM poles, Whiskers, and Heroes. Skiers and coaches from the Park City Ski Team, Summit Ski Team, and Bridger Ski Foundation for their help and participation.

References

1. Reid R, Gilgien M, Moger T et al (2009) Turn characteristics and energy dissipation in slalom. In: Müller E et al (eds) Science and Skiing IV. Meyer & Meyer Sport, Oxford, pp 419–429
2. FIS international ski competition rules book IV joint regulations for alpine skiing (2016) International Ski Federation FIS. Oberhofen, Switzerland
3. The International Ski Competition Rules (ICR) (2012) International Ski Federation FIS. Oberhofen, Switzerland
4. 2016 USSA Alpine Competition Guide (2015) U. S. Ski and Snowboard Association. Park City, UT
5. Schindelwig K, Kaps P, Nachbauer W (2015) Short and thin walled flex poles for children slalom race. In: Petrone N, Marcolin G (eds) 21st International Congress on Ski Trauma and Skiing Safety Book of Abstract, p 97

6. Belen'kii VY, Gurfinkel VS, Paltsev YI (1967) Elements of control of voluntary movements. Biofizika 12:135–141
7. Cordo P, Nashner L (1982) Properties of postural adjustments associated with rapid arm movements. J Neurophysiol 47:287–302
8. Page GD, Telford L, Seidman SH et al (1998) Human vestibuloocular reflex and its interactions with vision and fixation distance during linear and angular head movement. J Neurophysiol 80:2391–2404
9. Peterka RJ, Black FO, Schoenhoff MB (1990) Age-related changes in human vestibulo-ocular reflexes: sinusoidal rotation and caloric tests. J Vestib Res 1(1):49–59
10. Broussard DM, Kassardjian CD (2004) Learning in a simple motor system. Learn Mem 11:127–136
11. O'Brien MK, Ahmed AA (2016) Rationality in human movement. Exerc Sport Sci Rev 44(1):20–28
12. Pienciak-Siewert A, Barletta AJ, Ahmed AA (2013) Transfer of postural adaptation depends on context of prior exposure. J Neurophysiol 111:1466–1478
13. Manista GC, Ahmed AA (2012) Stability limits modulate whole-body learning. J Neurophysiol 107:1952–1961
14. Ekeland A, Rødven A (2009) Injury trends in Norwegian ski resorts in the 10 year period 1996–2006. In: Johnson RJ (ed) Skiing trauma and safety: 17th volume, ASTM STP 1510. American Society for Testing and Materials, West Conshohocken, PA, pp 31–38
15. Johnson RJ, Ettlinger CF, Shealy JE (2009) Updates on injury trends in alpine skiing. In: Johnson RJ, Shealy JE, Langran M (eds) Skiing trauma and safety: 17th volume. American Society for Testing and Materials, West Conshohocken, PA, pp 11–22
16. Fischer JF, Leyvraz PF, Bally A (1994) A dynamic analysis of knee ligament injuries in alpine skiing. Acta Orthop Belg 60:194–203
17. Ruedl G, Linortner I, Schranz A et al (2009) Distribution of injury mechanisms and related factors in ACL-injured female carving skiers. Knee Surg Sports Traumatol Arthrosc 17:1393–1398
18. Bare T (2011) Mechanisms of anterior cruciate ligament injury in world cup alpine skiing: a systematic video analysis of 20 cases. Am J Sports Med 39:1421–1429
19. PSIA Alpine Certification Standards (2014) ASEA and ASEA-EF. Lakewood CO
20. Kipp RW, Reid RC, Gilgien M et al (2008) Slalom performance in élite alpine ski racing can be predicted by fore/aft movement dynamics. Med Sci Sports Exerc 40(5):S1246
21. Kipp RW, Reid RC, Gilgien M et al (2009) Fore/aft movement is adapted to gate separation by elite alpine racers in slalom. In: 14th Annual Congress of the European College of Sports Science Book of Abstracts. Oslo, Norway, p 171

Auxetic Foam for Snow-Sport Safety Devices

Tom Allen, Olly Duncan, Leon Foster, Terry Senior, Davide Zampieri, Victor Edeh, and Andrew Alderson

Abstract Skiing and snowboarding are popular snow-sports with inherent risk of injury. There is potential to reduce the prevalence of injuries by improving and implementing snow-sport safety devices with the application of advanced materials. This chapter investigates the application of auxetic foam to snow-sport safety devices. Composite pads—consisting of foam covered with a semi-rigid shell—were investigated as a simple model of body armour and a large 70 × 355 × 355 mm auxetic foam sample was fabricated as an example crash barrier. The thermo-mechanical conversion process was applied to convert open-cell polyurethane foam to auxetic foam. The composite pad with auxetic foam absorbed around three times more energy than the conventional equivalent under quasi-static compression with a concentrated load, indicating potential for body armour applications. An adapted thermo-mechanical process—utilising through-thickness rods to control in-plane compression—was applied to fabricate the large sample with relatively consistent properties throughout, indicating further potential for fabrication of a full size auxetic crash barrier. Further work will create full size prototypes of snow-sport safety devices with comparative testing against current products.

Keywords Skiing • Padding • Impact protection • Snowboarding • Material

1 Introduction

Alpine skiing and snowboarding are popular Winter Olympic Sports. Worldwide participation numbers are hard to predict, but there are an estimated 115 to 200 million skiers [1, 2] and 10 to 15 million snowboarders [3–5]. Despite the popularity of snow-sports, there are inherent risks of injury, and even death. Snowboarders are at

T. Allen (✉)
Manchester Metropolitan University, Manchester, UK
e-mail: t.allen@mmu.ac.uk

O. Duncan • L. Foster • T. Senior • D. Zampieri • V. Edeh • A. Alderson
Sheffield Hallam University, Sheffield, UK
e-mail: A.Alderson@shu.ac.uk

I.S. Scher et al. (eds.), *Snow Sports Trauma and Safety*,
DOI 10.1007/978-3-319-52755-0_12

greater risk of injury than skiers [6–8], with estimates ranging from 1 to 15 injuries per 1,000 riding days [9, 10]. The upper extremities are particularly at risk among snowboarders [7, 9, 11, 12], with wrist injuries common for beginners and children [7, 13–16].

Falls account for the most snow-sport injuries, contributing to 43 to 73% of injuries for skiers and 69 to 93% of injuries for snowboarders [17]. Experienced participants experience the greatest incidence of injuries when attempting jumps [18]. Devices are available for reducing injuries; these include crash barriers and personal protective equipment (PPE). Crash barriers are often large foam pads, designed to limit peak force in the event of a collision with a fixed object. Personal protective equipment includes helmets, wrist protectors and body armour such as back protectors.

Standards ensure certified snow-sport helmets limit peak force (e.g. EN1077 [19] and ASTMF2040 [20]) and resist penetration (e.g. EN1077), but they do not always provide for protection against concussion [12]. There are no snow-sport-specific standards for wrist protectors [16] or back protectors [21]. There is consensus that wrist protectors can prevent injuries by absorbing energy and limiting hyperextension, but it is unclear which designs offer the most protection [16]. Back protectors come in two primary forms, a hard shell with padding underneath offering greater resistance to penetration, and foam in isolation which absorbs more impact energy [21]. Snow-sport safety devices might be improved through design changes including the application of advanced materials which could allow reduced bulk, increased comfort and greater protection across a range of scenarios.

A number of studies present a case for applying auxetic foam to sport safety devices [e.g. 22–26], and there are patents for sportswear with auxetic components [27–29]. Auxetic foams are characterised by a negative Poisson's ratio; when compressed in one direction these materials contract in one or more perpendicular directions. This contraction and densification under the region of contact can lead to increased indentation resistance [30], which could be particularly beneficial to snow-sport safety devices. The indentation resistance (H) for an isotropic material is related to Poisson's ratio (ν) and Young's modulus (E),

$$H \propto \left[\frac{\left(1-\nu^2\right)}{E}\right]^{-x} \tag{1}$$

where x depends on the indenter shape [31]. For isotropic materials, the thermodynamically allowable upper and lower limits for Poisson's ratio are +0.5 and −1.0, respectively. Hence, for a given Young's modulus, indentation resistance will have a maximum finite value when Poisson's ratio equals +0.5 for conventional (positive Poisson's ratio) materials, whereas it increases towards infinity as Poisson's ratio tends towards −1.0 for auxetic materials.

1.1 Auxetic Foam

Despite the wealth of research into auxetic foam, work is needed to determine how best to fabricate and apply it to snow-sport safety devices. The general mechanism involves compression of conventional foam, followed by softening and then stiffening in the compressed state to give a re-entrant cell structure, as outlined in Lakes [32]. Heating to around the "softening temperature" is the common method of softening ("thermo-mechanical softening") [e.g. 24, 32–35] although a chemical bath can also be used ("chemical–mechanical" or "mechanical–chemical–thermal softening") [36, 37]. Increasing volumetric compression ratio (VCR—ratio of uncompressed to compressed volume), up to a limit of approximately five, generally enhances auxetic behaviour and lowers Poisson's ratio [24, 33]. The conversion process can be applied to a range of materials [e.g. 34, 38], and highly anisotropic auxetic foam can be obtained by applying different amounts of compression in each direction during fabrication [39].

When applying the thermo-mechanical process, there is, as yet, no consensus regarding the best heating time and temperature combination to maximise auxetic behaviour. Differences may be due to variations in foam properties between studies, the VCR applied and the size of fabricated samples. Early exploratory studies produced small samples of auxetic foam [e.g. 32, 38], while recent work has produced larger samples as the research moves closer to commercial applications [23–25, 40, 41]. Producing large samples is challenging as the thermo-mechanical process can result in inhomogeneous auxetic foam due to non-uniform temperature and compression gradients present during fabrication [25, 33, 40, 42]. A reliable method of fabricating large volumes of auxetic foam is therefore required to facilitate production and testing for snow-sport safety applications, including monoliths for crash pads and sheets for body armour.

Auxetic behaviour is identified by confirmation of a negative Poisson's ratio. Poisson's ratio is often measured during low-speed stretching or compression, by tracking the position of markers on a sample followed by linear regression of lateral-strain vs. axial-strain data in the low axial-strain region [e.g. 25, 34]. Negative Poisson's ratios have been measured for auxetic foams subject to high-speed compression [24, 43]. This is especially relevant to snow-sport safety devices, which are typically required to absorb energy through compression at relatively high speed. Work exploring snow-sport safety applications of auxetic foams should, therefore, involve testing at high strains and strain rates, for both crash pads and body armour.

Auxetic foams have higher resilience [24, 32] and absorb more energy [44] under compression compared to their conventional open-cell counterparts. Their stress–strain curves have an extended quasi-linear region and the foam densifies earlier as a result of lateral contraction [34]. This lateral contraction can cause auxetic foam to deform less in the direction of the applied load under impact [23] and reduce peak force in comparison to conventional open-cell foam [23, 24]. Auxetic foams have been shown to be particularly effective at limiting forces from concentrated impact loads when combined with a semi-rigid shell [24, 25], which should lend them well to padding in body armour.

2 Objective

Auxetic foams offer potential to improve snow-sport safety devices, such as body armour or crash pads. Work is required to determine how best these novel materials can be utilised. This work will explore applications for body armour, by examining the energy absorbed by a composite pad consisting of an auxetic foam sheet and semi-rigid shell subject to a load–unload cycle. The feasibility of producing auxetic foam crash pads will be explored by applying an adapted thermo-mechanical process to fabricate a large sized sample.

3 Methods

Open-cell polyurethane foam (R30RF and R60RF, supplied by Custom Foams) was converted to auxetic foam. The foam has a working temperature range of −40 to +120 °C (as specified by the supplier), indicating it is suitable for use in typical climate conditions for snow-sports. Foam of the same type has been used in previous work [e.g. 24, 26] and similar thermo-mechanical conversion processes were adopted here. Over-sized foam samples were compressed in a metal mould consisting of two U-shaped parts, with the internal faces lubricated with olive oil. The mould containing the compressed foam was placed in an oven at 180 °C for two heating phases followed by a 20 min annealing phase at 100 °C. The heating time was dependent on the size of the foam sample. Each sample was removed from the mould after each phase and gently stretched by hand to reduce adhesion of cell ribs. Following annealing the foam was left to cool to room temperature in the mould. Poisson's ratio was measured from quasi-static tests by filming pins in a sample while it was being stretched or compressed. The video footage was analysed later with a Matlab (Mathworks) script, which automatically tracked the positions of the pins to obtain true strain. Details of the methods for the body armour and crash pad examples are described below.

3.1 Body Armour

Composites pads—consisting of a 10 × 90 × 90 mm or 20 × 90 × 90 mm foam sample covered with a 4 × 90 × 90 mm polypropylene (PP) sheet (Direct Plastics, PPH/PP-DWST-Homopolymer)—were investigated as a simple model of body armour. The larger pads had similar thickness to commercially available back protectors [21]. To help ensure uniform compression and temperature and the production of homogeneous samples, auxetic foam sheets were converted individually at the required thickness, rather than converting and then slicing a cube [26]. Foam (R30RF and R60RF) samples (15 × 143 × 143 mm and 30 × 143 × 143 mm) were

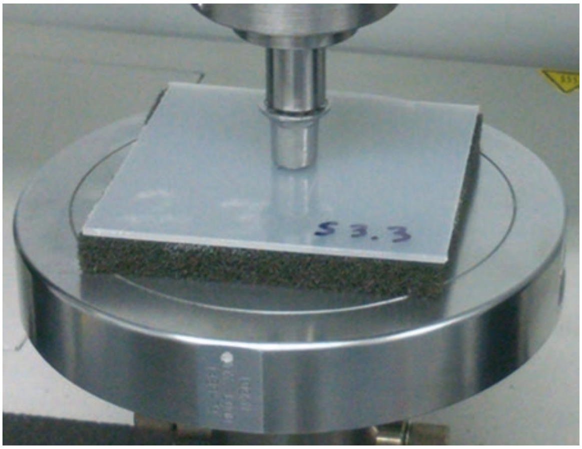

Fig. 1 Compression test set-up displaying foam sample, PP shell and stud used to apply a concentrated load

compressed to 70% of their original size along each dimension in a mould, resulting in a VCR of 3. The heating phases at 180 °C were 25 min long. After a week, a 5 mm wide strip was cut from each side of the foam cuboids to leave 10 × 90 × 90 mm or 20 × 90 × 90 mm samples. Thirteen samples were fabricated, six 10 mm thick and seven 20 mm thick. Two 10 × 90 × 90 mm and two 20 × 90 × 90 mm samples of unconverted foam (R60RF) were cut from a monolith for comparative testing.

Concentrated load compression testing (Instron 3369, fitted with a 50 kN load cell) was performed with a PP sheet placed unbonded on top of each sample. The pad rested on a flat plate and a load was applied to the centre of the upper face with a stud (Kipsta, aluminium football stud, 18 mm length) as shown in Fig. 1. Pilot testing confirmed the efficacy of the set-up for providing intermediate behaviour between compressing foam in isolation between two flat plates, and a stud and a flat plate. Following application of a small preload (approximately 1 N), the pad was compressed and unloaded in a cycle to 60% of the foam thickness (6 mm and 12 mm) at 3 mm/min. Energy absorbed was calculated as the difference between the area under the loading and unloading curve.

Chan and Evans [34] reported slightly lower Poisson's ratios for auxetic foam under tension in comparison to compression. In this work, Poisson's ratio was measured in tension to avoid issues with, (1) contact surface friction when compression testing thin sheets [24–26] and, (2) positioning and tracking pins in a small sample (cut from the sheet) under compression. After testing the pads, a sample of auxetic foam of each thickness and porosity was cut into three equal strips (resulting in six measuring 10 × 30 × 90 mm and six measuring 20 × 30 × 90 mm in total) and cardboard was glued to the ends so they could be gripped (Fig. 2). Each sample was stretched at 10 mm/min (strain rate of 0.002 s^{-1}) to 30% extension. Four pins in a 20 × 20 mm square in the face of the sample were filmed with a camera (JVC Everio Full HD resolution 1920 × 1080 pixels) and Poisson's ratio was obtained from linear regression of true lateral-strain vs. true axial-strain data up to 10% extension.

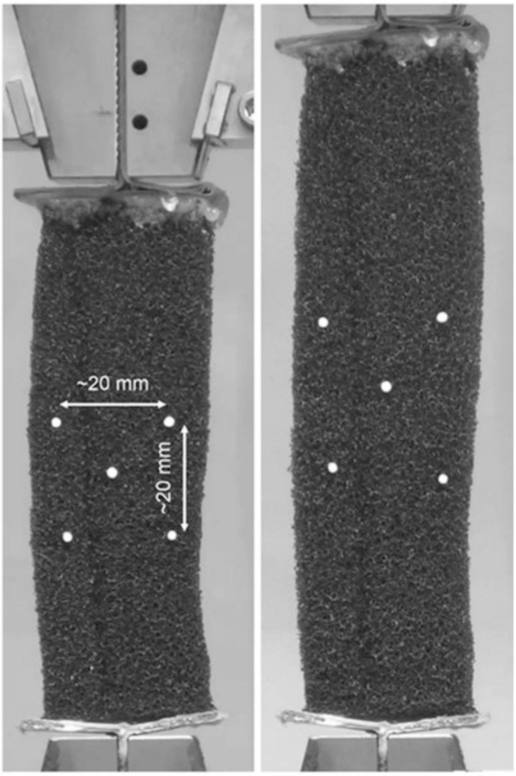

Fig. 2 Tensile test set-up displaying pins used to measure Poisson's ratio, (*Left)* no extension and (*Right*) maximum extension

3.2 Crash Pad

A 70 × 355 × 355 mm auxetic foam sample was created by compressing a 96 × 445 × 445 mm foam monolith into a mould with internal dimensions measuring 70 × 355 × 355, to give a VCR of 2. Through-thickness compression was marginally higher to account for elongated cells in the rise direction. Following the methods of Duncan et al. [26], through-thickness metal rods were used to help fit the foam into the mould, control in-plane compression and draw heat through the porous material (Fig. 3).

The face of each half of the mould contained a grid of 36 holes, with a diameter of 3.5 mm and an equal spacing of 50 mm (Fig. 3a). An equal number of rods with a diameter of 3 mm were inserted through the thickness of the uncompressed foam with 61 mm spacing (Fig. 3b). The rods passed through the corresponding holes in the two halves of the mould as they came together, helping to draw the foam into place (Fig. 3c, d). The heating phases at 180 °C were 35 min long, with the rods removed after the first and not returned. The dimensions of the sample were measured after cooling and then 7 days later to confirm the foam was stable and had not expanded.

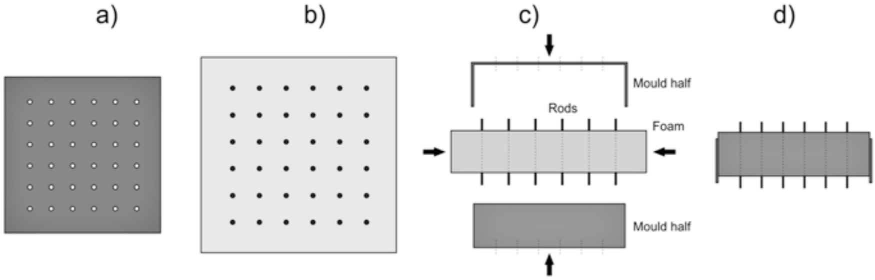

Fig. 3 Process used to fit the large foam sample into the mould, (**a**) top view of mould half with holes for rods, (**b**) top view of uncompressed foam with rods inserted, (**c**) illustration of foam compression into mould, and (**d**) side view of mould containing compressed foam with through-thickness rods

Three 50 × 50 × 70 mm samples were cut from the converted foam with a band-saw, corresponding to the centre, corner and centre of an edge (Fig. 4). Each sample was compressed (Instron 3367, fitted with a 5 kN load cell) three times between two flat plates along the longest dimension (70 mm) to 50% strain at 10 mm/min (strain rate of 0.002 s^{-1}). Pins in the face of the sample were filmed with a camera (Sony Handycam HFR-CX410 operating at 25 Hz) to obtain true strain (Fig. 5) in both directions. Two pins approximately midway up the sample and around 30 mm apart were used for true lateral-strain and four pins arranged in a rectangle around the centre were used for true axial-strain. Poisson's ratio was obtained from linear regression of the true lateral-strain vs. true axial-strain data up to 50% compression.

Density measurements of the samples were used to examine local variations in VCR and images of the foam were obtained with an optical microscope (Leica S6D) to examine cell structure.

4 Results

4.1 Body Armour

Figure 6a show lateral-strain vs. axial-strain from a tensile test of auxetic foam. Averaged across all 12 samples, mean Poisson's ratio was −0.01 with a standard deviation of 0.13, suggesting marginally auxetic behaviour. Figure 6b, c shows example force–displacement curves for concentrated load compression tests of pads. The pads containing conventional foam exhibited an initial region of high stiffness, followed by a plateau region with evidence of densification towards maximum compression. In contrast, pads containing auxetic foam exhibited an extended region of quasi-linear stiffness up to approximately 50% compression of the foam, followed by a region of increasing stiffness. The shape of these loading curves are similar to those reported for quasi-static compression testing of conventional and auxetic foam between two flat plates [32, 44].

Fig. 4 (**a**) Large (70 × 355 × 355 mm) sample of converted foam with samples removed and (**b**) 50 × 50 × 70 mm samples cut from large sample of converted foam

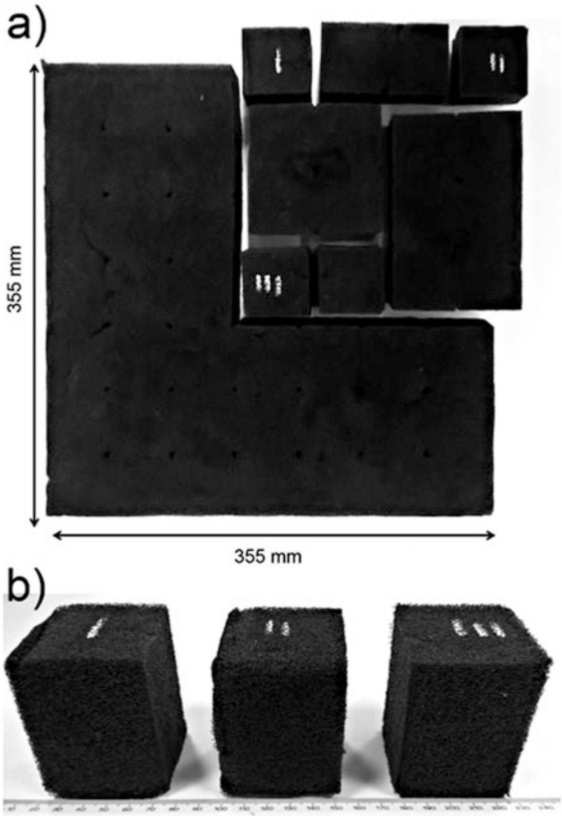

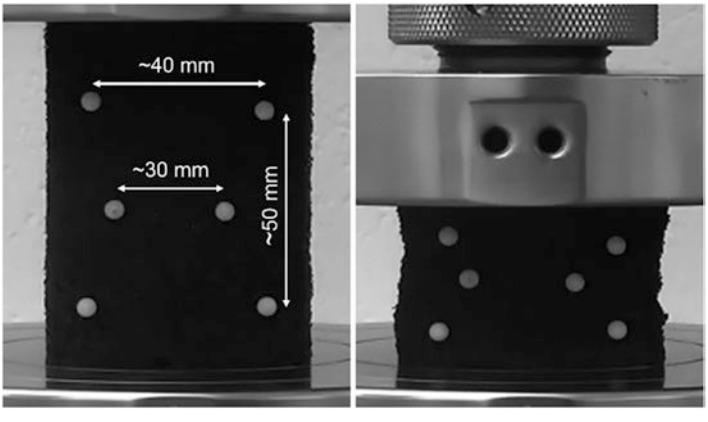

Fig. 5 Compression test set-up displaying pins used to measure Poisson's ratio, *Left*) No compression and *Right*) Maximum compression

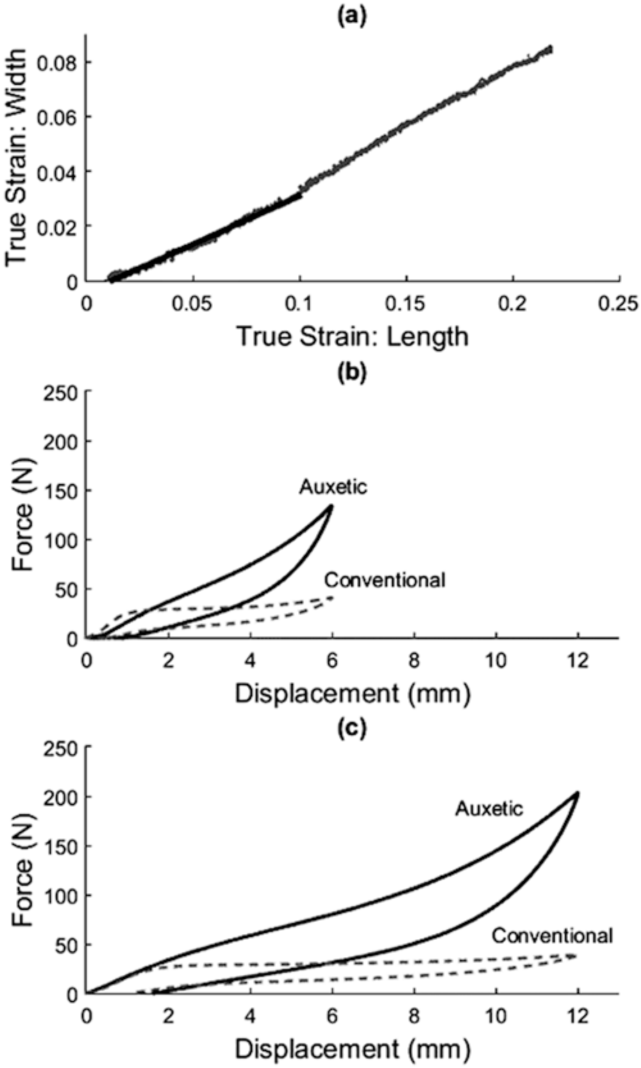

Fig. 6 (**a**) Strain–strain data for a tensile test on a 10 × 30 × 90 mm sample of R30RF auxetic foam, showing linear trend line used to obtain a Poisson's ratio of −0.4**.** Example force–displacement relationships for concentrated load quasi-static compression on composite pads consisting of an R60RF foam sheet and 4 mm thick polypropylene shell, (**b**) 10 mm thick foam and (**c**) 20 mm thick foam

Figure 7 summarises peak force and energy absorbed for the concentrated load compression tests on the pads. Peak force was approximately four times higher for the thin auxetic pads compared to their conventional counterparts and approximately five times higher for the thick auxetic pads than their conventional equivalents. For a given foam, the energy absorbed in the compression cycle increased with pad

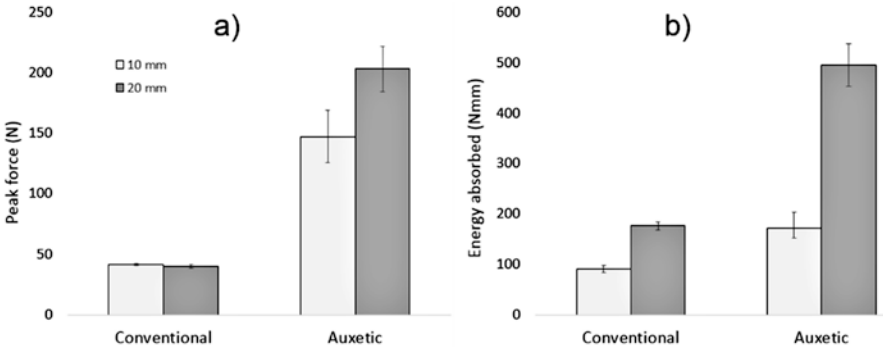

Fig. 7 Concentrated load compression testing results, (**a**) Peak force and (**b**) Energy absorbed. Error bars correspond to one standard deviation either side

thickness. The thinner pads with auxetic foam absorbed around twice as much energy as their unconverted counterparts, while the thicker auxetic pads absorbed approximately three times more energy than their conventional equivalents.

4.2 Crash Barrier

Figure 8a shows example compressive stress–strain curves for samples from the large foam conversion. The curves all show an extended quasi-linear region followed by progressive stiffening at approximately 30% compression, characteristic of auxetic foam [32, 35]. The corner sample was slightly stiffer above approximately 20% compression, with maximum stress ranging from 13 to 16 kPa in comparison to 11 to 13 kPa for the edge and centre samples. Figure 8b shows an example true lateral-strain vs. true axial-strain curve for the centre sample from the large foam conversion. Poisson's ratio was −0.078 ± 0.014 (mean ± standard deviation) for the corner sample, −0.013 ± 0.003 for the edge sample and −0.068 ± 0.010 for the centre sample, indicating marginally auxetic behaviour. Density measurements confirmed a VCR of approximately 2 for all samples. Figure 9 shows the conventional foam had a regular cell structure and all the converted foam samples had a re-entrant cell structure, characteristic of auxetic foam.

5 Discussion

Composite pads—consisting of a sheet of auxetic foam and a semi-rigid shell—absorbed approximately three times more energy than their conventional equivalent, under quasi-static compression with a concentrated load. Auxetic pads were also

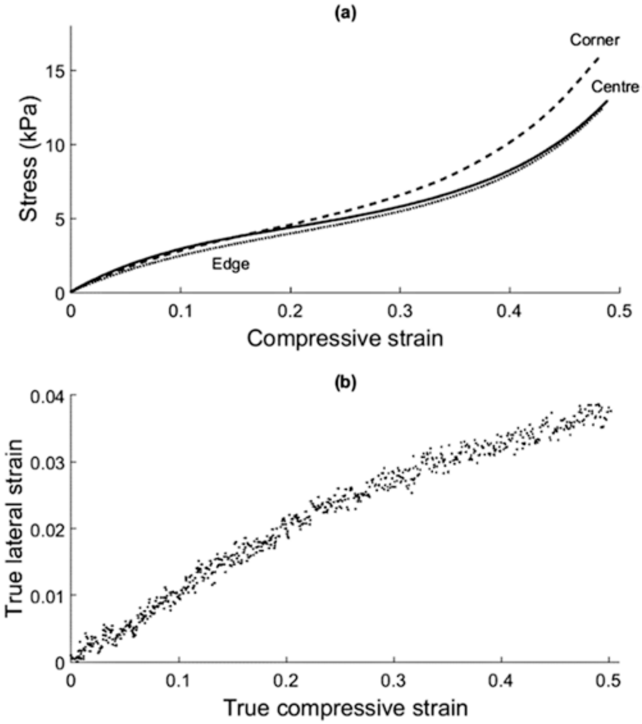

Fig. 8 (**a**) Example stress–strain relationship for quasi-static compression of 50 × 50 × 70 mm samples cut from the 70 × 355 × 355 mm sample of converted foam and (**b**) strain–strain relationship for the centre sample

stiffer with peak force approximately five times higher when compressed to 60% of the foam thickness, which will likely offer greater resistance to bottoming out under impact, as reported previously [24–26]. These results show further potential for auxetic foam as an energy-absorbing component in PPE for snow-sports, such as back or wrist protectors. Relatively low stiffness foam was used here and further work should aim to fabricate stiffer auxetic foam that is more representative of foam typically used in PPE.

A modified thermo-mechanical conversion process—utilising through-thickness rods to provide greater control over in-plane compression—was applied to produce a relatively large sample (70 × 355 × 355 mm) of auxetic foam as an example crash pad. Analysis of samples taken from different locations in the pad showed relatively consistent stress–strain curves, densities and Poisson's ratios, with a re-entrant cell structure throughout, indicating the new process can produce large quasi-homogeneous monoliths of auxetic foam. The new process can now be applied to produce samples with different VCRs, as the amount of compression during fabrication can influence impact performance [24]. Despite the relatively large size of the

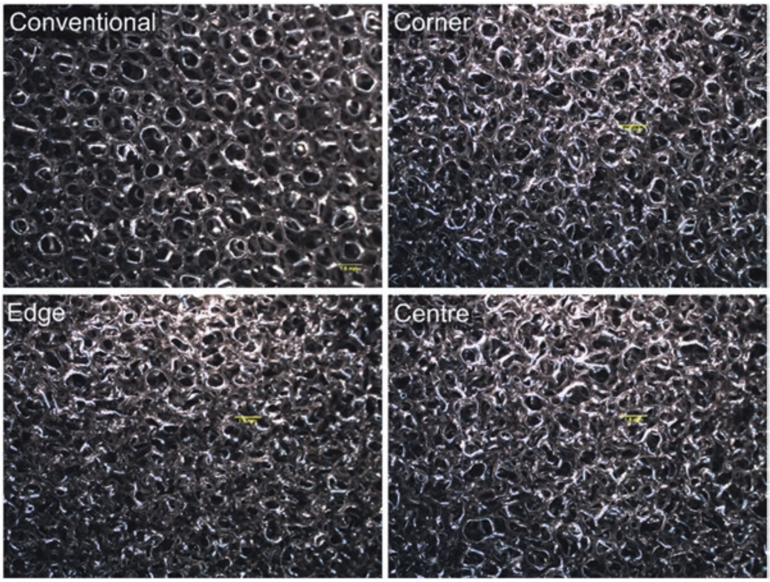

Fig. 9 Microscope images of cell structure for conventional foam and samples cut from the large conversion, (*Top left*) conventional foam, (*Top right*) Corner, (*Bottom left*) Edge, (*Bottom right*) Centre. The *yellow* scale line represents 1.5 mm

example auxetic pad in comparison to samples typically reported in the literature, it was smaller than a snow-sport safety crash barrier. Future work will, therefore, apply the new technique to produce a full size crash pad with comparative testing against current products.

Low temperature performance is important for snow-sport safety devices, and this needs careful consideration in further work investigating the application of auxetic foam. Different candidate foams should be investigated with a focus on identifying those with the most suitable working temperature range for snow-sports applications. EN1077 specifies snow-sports helmets to be acclimatised at both 20 °C and −25 °C prior to testing and a similar temperature range could be used as a starting point when characterising auxetic foam. Crash barriers will be repeatedly subject to extreme climate conditions on the mountain for extended periods of time, whereas body armour is typically worn underneath clothing where the minimum temperature should be higher. Future work should look towards identifying the most suitable candidate foams for specific applications.

The work presented here has shown further potential for auxetic foam to be applied to snow-sport safety devices. Future work will apply the new conversion process to produce larger sized samples, while tailoring mechanical properties of the auxetic foam to specific applications. Fabrication of prototypes and impact testing for scenarios representative of snow-sport collisions is required. Impact testing of auxetic foam should be performed at temperatures typical of those where snow-sport is practised and the effect of repeated loading should be investigated.

References

1. Hunter RE (1999) Skiing injuries. Am J Sports Med 27(3):381–389
2. Vanat L (2014) International report on snow & mountain tourism. http://www.vanat.ch/RM-world-report-2015.pdf. Accessed 22 Dec 2015
3. Dann K (2011) Snowboarding. In: Engelhardt M, Dorr A (eds) Sports orthopaedics. Elsevier, Official Manual of GOTS, pp 637–645
4. Hasler RM, Berov S, Benneker L et al (2010) Are there risk factors for snowboard injuries? a case-control multicentre study of 559 snowboarders. Br J Sports Med 44(11):816–821
5. Kusche H, Gutsfeld P, Bühren V (2010) Snowboarden. Sport Orthop Sport Traumatol 26(3):178–181
6. Hagel BE, Goulet C, Platt RW et al (2004) Injuries among skiers and snowboarders in Quebec. Epidemiology 15(3):279–286
7. Russell K, Hagel B, Francescutti LH (2007) The effect of wrist guards on wrist and arm injuries among snowboarders: a systematic review. Clin J Sport Med 17(2):145–150
8. Sasaki K, Takagi M, Ida H et al (1999) Severity of upper limb injuries in snowboarding. Arch Orthop Trauma Surg 119(5–6):292–295
9. Russell K, Hagel B, Goulet C (2010) Snowboarding. In: Caine DJ, Harmer PA, Schiff MA (eds) Epidemiology of injuries in olympic sports, vol XVI. Blackwell Publishing, Oxford, pp 447–472
10. Machold W, Kwasny O, Gäler P et al (2000) Risk of injury through snowboarding. J Trauma Acute Care Surg 48(6):1109–1114
11. Kim S, Lee SK (2011) Snowboard wrist guards-use, efficacy, and design: a systematic review. Bull NYU Hosp Jt Dis 69(2):149–157
12. Brügger O, Bianchi G, Schulz D et al (2010) Snow-sport helmets: injury prevention, rate of wearers and recommendations. Berne: bfu-Swiss Council for Accident Prevention. EuroSafe Task Force Safety in Sports
13. Matsumoto K, Sumi H, Sumi Y et al (2004) Wrist fractures from snowboarding: a prospective study for 3 seasons from 1998 to 2001. Clin J Sport Med 14:64–71
14. Torjussen J, Bahr R (2005) Injuries among competitive snowboarders at the national elite level. Am J Sports Med 33(3):370–377
15. Dickson TJ (2009) Risk factors in snowboarder's wrist fractures. In: Senner V, Fastenbauer V, Bohm H (eds) Proceedings of the 18th Congress of the International Society for Skiing Safety (ISSS). Technical University of Munich, Department of Sport Equipment and Materials, Garmisch-Partenkirchen, p 13
16. Michel FI, Schmitt KU, Greenwald RM et al (2013) White paper: functionality and efficacy of wrist protectors in snowboarding—towards a harmonized international standard. Sports Eng 16(4):197–210
17. Hagel B (2005) Skiing and snowboarding injuries. In: Caine DJ, Maffulli N (eds) Epidemiology of pediatric sports injuries, individual sports. Med sport sci, vol 48. Karger, Basel, pp 74–119
18. Hume PA, Lorimer AV, Griffiths PC et al (2015) Recreational snow-sports injury risk factors and countermeasures: a meta-analysis review and Haddon matrix evaluation. Sports Med 45(8):1–16
19. European Committee for Standardization (2007) Helmets for alpine skiers and snowboarders; EN 1077: 2007. EN 1077: 2007. European Committee for Standardization, Brussels

20. American Society for Testing and Materials (ASTM) (2002) ASTM F 2040-02: standard specification for helmets used for recreational snow sports. West Conshohocken
21. Schmitt KU, Liechti B, Michel FI et al (2010) Are current back protectors suitable to prevent spinal injury in recreational snowboarders? Br J Sports Med 44(11):822–826
22. Sanami M et al (2014) Auxetic materials for sports applications. In: James D, Choppin S, Allen T, Wheat J, Fleming P (eds) The Engineering of Sport 10, 10th Conference of the International Sports Engineering Association, Sheffield, July 2015, vol 72. Procedia Engineering, pp 453–458
23. Allen T et al (2015) Auxetic foams for sport safety applications. In: Subic A, Fuss FK, Alam F, Pang TY, Takla M (eds) The Impact of Technology on Sport VI. 7th Asia-Pacific Congress on Sports Technology, Barcelona, September 2015, vol 112. Procedia Engineering, pp 104–109
24. Allen T, Shepherd J, Hewage TAM et al (2015) Low-kinetic energy impact response of auxetic and conventional open-cell polyurethane foams. Phys Status Solidi B 252(7):1631–1639
25. Duncan O, Foster L, Senior T et al (2016) Quasi-static characterisation and impact testing of auxetic foam for sports safety applications. Smart Mater Struct 25(5):1–9
26. Duncan O, Foster L, Senior T, et al (2016) A comparison of novel and conventional fabrication methods for auxetic foams for sports safety applications. In: The Engineering of Sport 11. 11th Conference of the International Sports Engineering Association, Delft, July 2016, vol 147. Procedia Engineering, pp 384–389
27. Cross TM, Hoffer KW, Jones DP et al (2015) Auxetic structures and footwear with soles having auxetic structures. US patent 20,150,245,685, 3 Sep 2015
28. Bentham M, Alderson A, Alderson KL (2008) Garments having auxetic foam layers. US patent 7,455,567, 25 Nov 2008
29. Toronjo A (2013) Articles of apparel including auxetic materials. US Patent Application 13/838,827, filed 15 March 2013
30. Chan N, Evans KE (1998) Indentation resilience of conventional and auxetic foams. J Cell Plast 34(3):231–260
31. Evans KE, Alderson A (2000) Auxetic materials: functional materials and structures from lateral thinking! Adv Mater 12(9):617–628
32. Lakes R (1987) Foam structures with a negative Poisson’s ratio. Science 235(4792):1038–1040
33. Critchley R, Corni I, Wharton JA et al (2013) A review of the manufacture, mechanical properties and potential applications of auxetic foams. Phys Status Solidi B 250(10):1963–1982
34. Chan N, Evans KE (1999) The mechanical properties of conventional and auxetic foams. Part I: compression and tension. J Cell Plast 35(2):130–165
35. Scarpa F, Pastorino P, Garelli A et al (2005) Auxetic compliant flexible PU foams: static and dynamic properties. Phys Status Solidi B 242(3):681–694
36. Grima JN, Attard D, Gatt R et al (2009) A novel process for the manufacture of auxetic foams and for their re-conversion to conventional form. Adv Eng Mater 11(7):533–535
37. Lisiecki J, Błażejewicz T, Kłysz S et al (2013) Tests of polyurethane foams with negative Poisson's ratio. Phys Status Solidi B 250(10):1988–1995
38. Friis EA, Lakes RS, Park JB (1988) Negative Poisson’s ratio polymeric and metallic foams. J Mater Sci 23(12):4406–4414
39. Alderson A et al (2005) The effects of processing on the topology and mechanical properties of negative Poisson’s ratio foams. In: Proceedings of ASME International Mechanical Engineering Congress and Exposition (Aerospace Division), Orlando, Florida, November 2005, vol 70AD, p 503
40. Lowe A, Lakes RS (2000) Negative Poisson's ratio foam as seat cushion material. Cell Polym 19(3):157–168
41. Lisiecki J, Kłysz S, Błażejewicz T et al (2014) Tomographic examination of auxetic polyurethane foam structures. Phys Status Solidi B 251(2):314–320
42. Chan N, Evans KE (1997) Fabrication methods for auxetic foams. J Mater Sci 32(22): 5945–5953

43. Pastorino P, Scarpa FL, Patsias S et al (2007) Strain rate dependence of stiffness and Poisson's ratio of auxetic open cell PU foams. Phys Status Solidi B 244(3):955–965
44. Bezazi A, Scarpa F (2007) Mechanical behaviour of conventional and negative Poisson's ratio thermoplastic polyurethane foams under compressive cyclic loading. Int J Fatigue 29(5): 922–930